A common pattern of brain MRI imaging in mitochondrial diseases with complex I deficiency.

Anne-Sophie Lebre, Nathalie Boddaert

A COMMON PATTERN OF BRAIN MRI IMAGING IN MITOCHONDRIAL DISEASES WITH COMPLEX I DEFICIENCY

AS Lebre[1], PhD, Mitochondrial diseases study group[£], A Munnich[1] MD, PhD, N Boddaert[1] MD, PhD.

[£] M Rio[1] MD, PhD , L Faivre d'Arcier[1] MD, D Vernerey[1*], P Landrieu[2] MD, A Slama[2] MD, C Jardel[3] MD, P Laforêt[3] MD, D Rodriguez[4] MD, N Dorison[4] MD, D Galanaud[3] MD, B Chabrol[5] MD, V Paquis-Flucklinger[6] MD, PhD, D Grévent[1] MD, S Edvardson[7] MD, J Steffann[1] MD, PhD, B Funalot[8] MD, PhD, N Villeneuve[5] MD, V Valayannopoulos[1] MD, P de Lonlay[1] MD, PhD, I Desguerre[1] MD, F Brunelle[1] MD, PhD, JP Bonnefont[1] MD, PhD, A Rötig[1], PhD constitute additional members of the Mitochondrial diseases study group

Correspondence to Dr Anne-Sophie Lebre, PhD, Hôpital Necker-Enfants Malades, Département de Génétique, Bâtiment Lavoisier 3[è] étage, 149 rue de Sèvres, 75015 Paris, France. anne-sophie.lebre@nck.aphp.fr; tel: +33 1 44 49 51 64, fax: +33 1 71 19 64 20)

1 Université Paris Descartes, AP-HP Hôpital Necker-Enfants Malades et Inserm U781 et U797, Départements de Génétique, de Radiologie pédiatrique et des Maladies du développement, Paris F-75015 France

2 Université Paris XI, AP-HP Hôpital Bicêtre, Départements de Neurologie pédiatrique et de Biochimie, Kremlin-Bicêtre F-94270 France

3 AP-HP Hôpital Pitié-Salpêtrière, Départements de Biochimie et de Radiologie et Institut de myologie, Paris F-75013 France

4 UPMC Univ Paris 06, AP-HP Hôpital Armand Trousseau-La Roche-Guyon et Inserm UMR 975, Département de Neuropédiatrie, Paris F-75012, France

5 Université de Marseille, AP-HM Hôpital de la Timone-Enfants, Départements de Neurologie et de pédopsychiatrie pédiatrique, Marseille F-13000, France

6 Université de Nice Sophia Antipolis, Hôpital Archet 2, Département de Génétique Médicale, Nice F-06000, France.

7 Pediatric Neurology, Hadassah Hebrew University Medical Center, Jerusalem, Israel.

8 Université de Limoges, Hôpital Universitaire Dupuytren, Département de Neurologie, Limoges F-87000, France

* conducted the statistical analysis

KEY WORDS : Mitochondrial disorders; Leigh syndrome; MRI; complex I deficiency

WORDS COUNT: 1873

ABBREVIATIONS:

RC: respiratory chain, LS: Leigh syndrome, LHON: Leber Hereditary Optic Neuropathy, PDH: Pyruvate dehydrogenase, MELAS: Mitochondrial Encephalomyopathy, Lactic Acidosis and Stroke-like episodes, INAD: infantile neuroaxonal dystrophy, mtDNA: mitochondrial DNA, nDNA: nuclear DNA, MRI: Magnetic Resonance Imaging, MRS: magnetic Resonance spectroscopy, CT: computed tomography, FLAIR: fluid-attenuated inversion recovery, CACH: childhood ataxia with central nervous system hypomyelination, MLC: megalencephalic leukodystrophy with subcortical cysts, AGS: Aicardi-Goutières syndrome

ABSTRACT:

Objective: To identify a consistent pattern of brain MRI imaging in primary complex I deficiency. Complex I deficiency, major cause of respiratory chain dysfunction, accounts for various clinical presentations, including Leigh syndrome. Human complex I comprises seven core subunits encoded by mitochondrial DNA (mtDNA) and 38 core subunits encoded by nuclear DNA (nDNA). Moreover, its assembly requires six known and many unknown assembly factors. To date, no correlation between genotypes and brain MRI phenotypes has been found in complex I deficiencies.

Design and Subjects: We have retrospectively collected the brain MRIs of 30 patients carrying known mutation(s) in genes involved in complex I and compared them with the brain MRIs of 11 patients carrying known mutations in genes involved in the pyruvate dehydrogenase (PDH) complex as well as 10 patients with *MT-TL1* mutations.

Results: All complex I deficient patients showed bilateral brainstem lesions (30/30) and 77% (23/30) showed anomalies of the putamen. Supra-tentorial stroke-like lesions were only observed in complex I-deficient patients carrying mtDNA mutations (8/19) and necrotizing leukoencephalopathy in patients with nDNA mutations (4/5). Conversely, the isolated stroke-like images observed in patients with *MT-TL1* mutations, or the corpus callosum malformations observed in PDH-deficient patients, were never observed in complex I-deficient patients.

Conclusion: We identified a common pattern of brain MRI imaging with abnormal signal intensities in brainstem and subtentorial nuclei with lactate-peak as a clue of complex I deficiency. We suggest that combining clinico-biochemical data with brain imaging can help orient genetic studies in complex I deficiency.

INTRODUCTION

Isolated complex I deficiency, the most frequent cause of respiratory chain defects in childhood [1], accounts for various clinical presentations including Leigh Syndrome, Leber Hereditary Optic Neuropathy (LHON), Mitochondrial Encephalomyopathy, Lactic Acidosis and Stroke-like episodes (MELAS) and numerous other clinical presentations combining hypotonia, developmental delay, seizures, cardiomyopathy, optic atrophy or retinopathy and other organ involvement [2].

Complex I (NADH:ubiquinone oxidoreductase; EC 1.6.5.3), the largest component of the respiratory chain, comprises seven core subunits encoded by mitochondrial DNA (mtDNA), 38 core subunits encoded by nuclear DNA (nDNA) and a few known (but many unknown) assembly factors [1, 2]. To date, disease-causing mutations have been identified in 19 core subunits, including twelve nuclear genes (*NDUFS1-4, NDUFS6-8, NDUFV1-2, NDUFA1-2* and *NDUFA11*), seven mtDNA genes and six assembly factors (*NDUFAF1-4, C8orf38* and *C20orf7*)[3].

While MRI abnormalities have been reported in patients with respiratory chain disorders, including those presenting complex I deficiency, no correlation between genotypes and brain MRI phenotypes has been hitherto reported in a large series of patients.

We have retrospectively collected brain MRI and/or CT-scan of 30 complex I deficient patients carrying known mutations and compared them with the brain MRI of 11 patients with known mutations in pyruvate dehydrogenase (PDH) genes and 10 patients with *MT-TL1* mutations. This retrospective study allows us to identify a consistent pattern of brain MRI imaging in primary complex I deficiency.

PATIENTS AND METHODS

Patients

A total of 30 patients with complex I deficiency (25 males, 5 females) were included in this study. Inclusion criteria were i) known mutation(s) in either mtDNA or nuclear genes, ii) availability of brain imaging for review. The mean age at imaging ranged from to 2 months to 30 years (mean = 6.8 years). Their brain MRIs were compared to those of 11 patients (8 males, 3 females) with known PDH mutation(s) and 10 patients (5 males, 5 females) with *MT-TL1* mutation (m.3243A>G or m.3271T>C). Mean ages at imaging ranged from to 4 months to 9 years (mean = 4.08 years) and from 4 years to 56 years (mean = 21.9 years) for PDH-deficient patients and for patients with *MT-TL1* mutations respectively. Clinical and biochemical features have been previously reported in 31 patients [4-14]. Written informed consent was obtained from all patients participating in the study. All reported mutations are described in Mitomap (http://www.mitomap.org/MITOMAP) and HGMD (https://portal.biobase-international.com/) databases.

Brain imaging methods

The MRI examination consisted of sagittal spin echo (SE) T1, axial fast SE (FSE) T2 and coronal fluid-attenuated inversion recovery (FLAIR) images. Additional imaging sequences were occasionally obtained, including 3D fast spoiled gradient recalled imaging (FSPGR), T2*, diffusion weighted images, 1H magnetic resonance spectroscopy (MRS) or one of the primary sequences in additional planes. MRS single voxel spectroscopy was most commonly performed using PRESS TR=1500 and TE=144; TE=288 was occasionally employed. The patients had one spectroscopy in their basal ganglia and eventually one in their brain anomalies. Exceptionally, brain MRI was performed with an injection of contrast. MRIs were acquired with a 1 or 1.5-Tesla Signa GE. For the majority of patients, scans were all collected on the same MRI scanner with the same protocol. For a few patients, brain MRIs had been performed many years ago or in other hospitals. Missing images or data were reported as non available (na). CT-scan was the only available brain images for two complex

I-deficient patients and for four patients with *MT-TL1* mutations. The same paediatric neuroradiologist reviewed all brain images.

Statistical calculations were performed with R version 2.8.0 (The R Foundation for Statistical Computing). Qualitative variables were compared by the chi^2 (χ^2) or the Fisher exact tests and quantitative variables were compared using the Students t-test. Statistical significance was defined as $p < 0.05$. All statistical tests were two sided.

RESULTS

Among our 30 complex I-deficient patients, 20 carried a mtDNA mutation and ten, a nuclear gene mutation (Tables 1-2). Brain MRI anomalies were consistently observed in the brainstem of all patients (Tables 1-2). Hyperintensities in the brainstem were found on T2 and FLAIR sequences (Fig 1) and appeared as hypointensities on T1. They were very important in size and generally symmetrical. Confluent areas of hyperintensitiy were occasionally seen. Substantia nigra, periaqueductal gray matter and mamillothalamic and spinothalamic tracts and/or medial lemniscus, medial longitudinal fasciculus were occasionally involved. Subthalamic nuclei, periaqueductal gray matter and superior colliculus lesions were more frequently observed in patients carrying mtDNA than nuclear mutations (data not shown).

Brainstem lesions were associated with at least one striatal anomaly (putamen or caudate) in 27/30 patients. No patient presented thalamus anomalies without striatal lesions. Striatal anomalies were almost consistently present (27/30, 90%) independent of the mutated genome. Putamenal (23/30, 77%) and pallidal lesions (16/30, 53%) were frequent as well regardless the mutation. Caudate lesions were frequently present (11/30, 37%) and were more common in patients with mtDNA as opposed to nuclear mutations (10/20, 50% and 1/10, 10% respectively) ($p < 0.05$).

Interestingly, stroke-like lesions predominantly affecting gray matter and not confined to arterial vascular territories were observed in 40% of patients carrying mtDNA mutations (8/20) but in none of the patients carrying nDNA mutations ($p < 0.05$) (Fig 2A-C).

A diffuse supratentorial leukoencephalopathy involving the deep lobar white matter was observed in 50% of patients with nDNA mutations (5/10) but in none of the patients carrying mtDNA mutations. The leukoencephalopathy was most likely necrotizing in 4/5 patients, including 3/4 patients with *NDUFS1* mutations. FLAIR sequences were available for 2/4 patients with abnormal white matter containing cysts (Fig 2D). In the 2/4 others patients, lesions were markedly hyperintense on T2 and very hypointense on T1 weighted images, suggesting cysts (Fig 2E-F).

Cerebellar hyperintensities were present in 13/29 patients (45%) regardless the mutated genome. Cerebellar atrophy was observed in 9/12 patients carrying mtDNA mutation aged 5 years (75%) but neither below five years nor in patients carrying nDNA mutations.

Spinal cord was not usually explored but T2 hyperintensities were observed in all three cases studied. When magnetic resonance spectroscopy (MRS) was performed and voxels placed over the brain lesions, important lactate peaks were consistently found in all patients (10/10), independent of the type of mutation (mtDNA or nDNA).

Patients with nDNA mutations presented significantly earlier brain anomalies than patients with mtDNA mutations (2.8 years and 8.9 respectively, $p < 0.05$).

A group of 11 PDH-deficient patients and 10 patients with *MT-TL1* mutations was chosen as control group (Tables 3-4). MRI anomalies in complex I-deficient patients were observed significantly earlier than in patients with *MT-TL1* mutations (mean age: 6.8 years versus 21.9 years, $p<0.05$). Similarly, brainstem lesions associated with at least one striatal anomalies were significantly more frequent in complex I-deficient patients (27/30) than in PDH-deficient patients (1/11, $p<0.001$) and were never observed in patients with *MT-TL1* mutations (0/6, $p<0.001$). Interestingly, stroke-like lesions were equally frequent in patients carrying complex I mtDNA mutations (8/20) and in patients with *MT-TL1* mutations (5/11) but were never observed in PDH deficient patients. Similarly, brainstem anomalies associated with stroke-like images or leukoencephalopathy were common in complex I deficiency but were never observed in PDH deficient patients or patients with *MT-TL1* mutations.

Cerebellar hyperintensities were observed in all groups. Cerebellar atrophy before five years was observed in PDH deficient patients (3/7) but not in complex I deficient patients (0/16, $p<0.05$). Similarly anomaly of the corpus callosum was very frequent in PDH deficient patients (9/10) but never observed in complex I deficient children (0/30, $p>0.001$). When available, CT-scan showed calcifications in basal ganglia in patients with *MT-TL1* mutations (6/6) but not in complex I deficient patients (0/3, $p<0.05$).

DISCUSSION

Based on a retrospective study of 30 cases, we report here on a common pattern of brain MRI imaging in patients with mitochondrial diseases and respiratory chain complex I deficiency. Bilateral and symmetric brainstem lesions were consistent features in complex I deficiency and most patients also presented at least one associated striatal anomaly. This association was significantly more frequent in complex I-deficient patients (27/30) than in PDH-deficient patients (1/11) or patients with *MT-TL1* mutations (0/6)($p<0.001$, Tables 3-4)[14]. The almost consistent detection of a lactate peak in our series supports the view that MRS should be performed in all patients with suspected complex I deficiency.

Abnormal brain images were observed significantly earlier in patients with nDNA mutations than in patients with mtDNA mutations. The age at onset was not determined by the date of the brain imaging; however, this could suggest an earlier clinical presentation for patients with nDNA mutations. For mtDNA mutations, heteroplasmic load has been shown to correlate with age at onset [15]. In this retrospective study, samples were not available anymore to quantify it. However, heteroplasmic load may contribute to explain later diagnosis for patients with mtDNA mutation (compared to patients with nDNA mutations) and the differences in brain image findings in patients with a same mtDNA mutation.

Supra-tentorial stroke-like lesions, similar to that observed in *MT-TL1* [16], *CABC1* [17] or *POLG* [18] mutations, were only observed in patients with mtDNA mutations. CT-scans showed no evidence of calcifications in these patients with stroke-like lesions. As brainstem lesions are usually not observed in patients with mutations in *MT-TL1* [16] (Table 3), *CABC1* [17] or *POLG* [18], the combination of brainstem anomalies with stroke-like images, but without calcifications, should help focusing on the mtDNA-encoded complex I genes. In contrast, stroke-like images with calcifications and without brainstem anomalies should prompt to screen for *MT-TL1* mutations [19].

In this study, necrotizing leukoencephalopathy was found in patients carrying nuclear genes mutations as already described in *NDUFA12L* [20] and *C6ORF66* [21] mutations. This suggests that a necrotizing leukoencephalopathy in patients with complex I deficiency should first prompt to investigate nuclear genes including the *NDUFS1*, *NDUFS3*, *NDUFS7*, *NDUFA12L* and *C6ORF66* genes. Brain MRI also help diagnosing other causes of necrotizing leukoencephalopathy namely childhood ataxia with central nervous system hypomyelination (CACH), megalencephalic leukodystrophy with subcortical cysts (MLC) and Aicardi-Goutières syndrome (AGS) [22].

Apart from complex I deficiency, brain MRI involvement of brainstem and basal ganglia anomalies have also been reported in cases of Leigh syndromes ascribed to *SURF1* and *MT-ATP6* mutations [23-28]. Similarly, brain MRI imaging of patients carrying *RanBP2* mutations is relatively similar to that observed in LS patients and reportedly includes brainstem and thalamus lesions [29]. Yet, reported *RanBP2* patients never presented the striatal anomalies that are constantly observed in our complex I deficient patients. Therefore the presence of striatal anomalies may help to distinguish between the two diagnoses.

Magnetic resonance spectroscopy (MRS) data were obtained only in 10/30 patients and an important lactate peak was consistently found in all patients. MRS is usually regarded as a more sensitive tool than CSF lactate [30]. For this reason, MRS should explore brainstem or white matter (in case of leukoencephalopathy) in complex I deficiency.

In conclusion, this retrospective study supports the view that mutations in complex I genes cause a common pattern of brain MRI imaging. We suggest giving consideration to association of brainstem and basal ganglia anomalies with lactate peak but no corpus callosum dysmorphism as a clue of complex I deficiency. When associated with stroke-like lesions or cerebellar atrophy, these images should prompt to screen for mtDNA mutations. Finally, a necrotizing leukoencephalopathy should prompt to look for nuclear genes mutations.

Hence, brain imaging may help focusing on specific genes and contribute to faster gene identification in respiratory chain deficiency.

TABLES AND FIGURES LEGENDS

Table 1: Neuroradiological and molecular genetic findings in 30 patients with complex I deficiency

Table 2: Comparative neuroradiological findings in 30 patients with primary complex I deficiency

Table 3: Neuroradiological and molecular genetic findings in 11 patients with PDH deficiency and 10 patients with *MT-TL1* mutations

Table 4: Comparative neuroradiological findings in 30 patients with primary complex I deficiency, 11 patients with PDH deficiency and 10 patients with *MT-TL1* mutations

Figure 1: Characteristic brain MRI. Characteristic brain MRI pattern of primary complex I deficiency (patient 1 with *ND3* mtDNA mutation at the age of 4 months).

(A) Axial T2-weighted images show important bilateral hyperintensities in the brainstem (white arrows). (B) Axial T2-weighted images show hyperintensities in the lenticular nuclei and thalami (black arrows). (C) MRS spectroscopy (TE 144) of lenticular nuclei shows a lactate peak at 1.33 ppm (white arrow).

Figure 2: Stroke-like and leukoencephalopathy images (axial FLAIR in A-D and T2-weighted images in E-F in absence of FLAIR images for patients 23-24).

(A-C) Multiple stroke-like images (indicated with white stars) associated with basal ganglia hyperintensities (white arrows) in two cases (patient 2 with *MT-ND3* in A-B; patient 14 with *MT-ND5* in C). (D-F) Necrotizing or cystic leukoencephalopathy images (patient 29 with *NDUFS7* mutations in D; patients 23 and 24 with *NDUFS1* mutations in E-F). Leukoencephalopathy is indicated with black arrows. White matter cerebellar hyperintensities are indicated with a white star.

ACKNOWLEDGMENTS

We thank Dr. Michèle Brivet (Hôpital Bicêtre, Service de Biochimie France) for providing us informations on PDH patients. We are grateful to all patients, doctors, nurses, and other people who were involved with the series studies.

COMPETING INTERESTS : none

FUNDING: This work is supported by the Mitocircle contract from the European commission [grant No 005260].

REFERENCES

1. Smeitink J, van den Heuvel L, DiMauro S. The genetics and pathology of oxidative phosphorylation. *Nat Rev Genet* 2001;**2**(5):342-52.
2. Loeffen JL, Smeitink JA, Trijbels JM, *et al.* Isolated complex I deficiency in children: clinical, biochemical and genetic aspects. *Hum Mutat* 2000;**15**(2):123-34.
3. Saada A, Vogel RO, Hoefs SJ, *et al.* Mutations in NDUFAF3 (C3ORF60), encoding an NDUFAF4 (C6ORF66)-interacting complex I assembly protein, cause fatal neonatal mitochondrial disease. *Am J Hum Genet* 2009;**84**(6):718-27.
4. Benit P, Chretien D, Kadhom N, *et al.* Large-scale deletion and point mutations of the nuclear NDUFV1 and NDUFS1 genes in mitochondrial complex I deficiency. *Am J Hum Genet* 2001;**68**(6):1344-52.
5. Benit P, Slama A, Cartault F, *et al.* Mutant NDUFS3 subunit of mitochondrial complex I causes Leigh syndrome. *J Med Genet* 2004;**41**(1):14-7.
6. Lebon S, Minai L, Chretien D, *et al.* A novel mutation of the NDUFS7 gene leads to activation of a cryptic exon and impaired assembly of mitochondrial complex I in a patient with Leigh syndrome. *Mol Genet Metab* 2007;**92**(1-2):104-8.
7. Lebon S, Rodriguez D, Bridoux D, *et al.* A novel mutation in the human complex I NDUFS7 subunit associated with Leigh syndrome. *Mol Genet Metab* 2007;**90**(4):379-82.
8. Benit P, Beugnot R, Chretien D, *et al.* Mutant NDUFV2 subunit of mitochondrial complex I causes early onset hypertrophic cardiomyopathy and encephalopathy. *Hum Mutat* 2003;**21**(6):582-6.
9. Chol M, Lebon S, Benit P, *et al.* The mitochondrial DNA G13513A MELAS mutation in the NADH dehydrogenase 5 gene is a frequent cause of Leigh-like syndrome with isolated complex I deficiency. *J Med Genet* 2003;**40**(3):188-91.
10. Lebon S, Chol M, Benit P, *et al.* Recurrent de novo mitochondrial DNA mutations in respiratory chain deficiency. *J Med Genet* 2003;**40**(12):896-9.
11. Sarzi E, Brown MD, Lebon S, *et al.* A novel recurrent mitochondrial DNA mutation in ND3 gene is associated with isolated complex I deficiency causing Leigh syndrome and dystonia. *Am J Med Genet A* 2007;**143**(1):33-41.
12. Pagniez-Mammeri H, Lombes A, Brivet M, *et al.* Rapid screening for nuclear genes mutations in isolated respiratory chain complex I defects. *Mol Genet Metab* 2009;**96**(4):196-200.
13. Leshinsky-Silver E, Lebre AS, Minai L, *et al.* NDUFS4 mutations cause Leigh syndrome with predominant brainstem involvement. *Mol Genet Metab* 2009;**97**(3):185-9.
14. Barnerias C, Saudubray JM, Touati G, *et al.* Pyruvate dehydrogenase complex deficiency: four neurological phenotypes with differing pathogenesis. *Dev Med Child Neurol* 2009.
15. Distelmaier F, Koopman WJ, van den Heuvel LP, *et al.* Mitochondrial complex I deficiency: from organelle dysfunction to clinical disease. *Brain* 2009;**132**(Pt 4):833-42.

16. Valanne L, Ketonen L, Majander A, *et al*. Neuroradiologic findings in children with mitochondrial disorders. *AJNR Am J Neuroradiol* 1998;**19**(2):369-77.
17. Mollet J, Delahodde A, Serre V, *et al.* CABC1 gene mutations cause ubiquinone deficiency with cerebellar ataxia and seizures. *Am J Hum Genet* 2008;**82**(3):623-30.
18. Kollberg G, Moslemi AR, Darin N, *et al.* POLG1 mutations associated with progressive encephalopathy in childhood. *J Neuropathol Exp Neurol* 2006;**65**(8):758-68.
19. Haas R, Dietrich R. Neuroimaging of mitochondrial disorders. *Mitochondrion* 2004;**4**(5-6):471-90.
20. Ogilvie I, Kennaway NG, Shoubridge EA. A molecular chaperone for mitochondrial complex I assembly is mutated in a progressive encephalopathy. *J Clin Invest* 2005;**115**(10):2784-92.
21. Saada A, Edvardson S, Rapoport M, *et al*. C6ORF66 is an assembly factor of mitochondrial complex I. *Am J Hum Genet* 2008;**82**(1):32-8.
22. Schiffmann R, Boespflug-Tanguy O. An update on the leukodsytrophies. *Curr Opin Neurol* 2001;**14**(6):789-94.
23. Rahman S, Brown RM, Chong WK, *et al*. A SURF1 gene mutation presenting as isolated leukodystrophy. *Ann Neurol* 2001;**49**(6):797-800.
24. Savoiardo M, Zeviani M, Uziel G, *et al.* MRI in Leigh syndrome with SURF1 gene mutation. *Ann Neurol* 2002;**51**(1):138-9.
25. Farina L, Chiapparini L, Uziel G, *et al.* MR findings in Leigh syndrome with COX deficiency and SURF-1 mutations. *AJNR Am J Neuroradiol* 2002;**23**(7):1095-100.
26. Rossi A, Biancheri R, Bruno C, *et al*. Leigh Syndrome with COX deficiency and SURF1 gene mutations: MR imaging findings. *AJNR Am J Neuroradiol* 2003;**24**(6):1188-91.
27. Bianchi MC, Sgandurra G, Tosetti M, *et al.* Brain magnetic resonance in the diagnostic evaluation of mitochondrial encephalopathies. *Biosci Rep* 2007;**27**(1-3):69-85.
28. Rojo A, Campos Y, Sanchez JM, *et al.* NARP-MILS syndrome caused by 8993 T>G mitochondrial DNA mutation: a clinical, genetic and neuropathological study. *Acta Neuropathol* 2006;**111**(6):610-6.
29. Neilson DE, Adams MD, Orr CM, *et al*. Infection-triggered familial or recurrent cases of acute necrotizing encephalopathy caused by mutations in a component of the nuclear pore, RANBP2. *Am J Hum Genet* 2009;**84**(1):44-51.
30. Boddaert N, Romano S, Funalot B, *et al*. 1H MRS spectroscopy evidence of cerebellar high lactate in mitochondrial respiratory chain deficiency. *Mol Genet Metab* 2008;**93**(1):85-8.

Table 1

						Brain imaging anomalies																			
Patient	Age at brain imaging	Sex (M/F)	Gene	Mutation	CT-Scan/MRI	brainstem	putamen	caudate	pallidum	thalamus	calcifications in basal ganglia	dilated wirshow robin in basal ganglia	leukoencephalopathy	necrotizing leukoencephalopathy	delayed myelination	stroke-like	cortical atrophy	cerebellum: hypersignal in cortex	cerebellum: hypersignal in dentate nucleus	cerebellum: hypersignal in white matter	cerebellar cortex atrophy	corpus callosum dysmorphy	Spinal cord	lactate (MRS)
1	4 mo	F	*MT-ND3*	m.10158T>C	MRI	+	+	-	+	+	(£)	-	-	-	-	-	-	-	-	-	-	-	np	+
2	7,5 y	M	*MT-ND3*	m.10158T>C	MRI	+	+	+	-	-	(£)	-	-	-	-	+	-	-	-	-	+	-	np	+
3	7 mo	M	*MT-ND3*	m.10191T>C	MRI	+	+	-	-	+	(£)	-	-	-	-	-	+	-	-	-	-	-	np	+
4	4 y	M	*MT-ND3*	m.10191T>C	MRI	+	+	+	+	+	(£)	-	-	-	-	+	-	-	-	-	-	-	np	np
5	8 y	M	*MT-ND3*	m.10191T>C	MRI	+	+	-	+	-	(£)	-	-	-	-	+	-	+	+	+	+	-	np	np
6	13 y	F	*MT-ND3*	m.10191T>C	MRI	+	+	+	-	+	(£)	-	-	-	-	+	+	+	+	+	+	-	np	np
7	19 y	M	*MT-ND3*	m.10191T>C	MRI	+	+	+	-	-	(£)	-	-	-	-	-	+	-	-	-	+	-	np	np
8	6 mo	M	*MT-ND3*	m.10197G>A	MRI	+	+	-	+	+	(£)	-	-	-	-	+	+	-	-	-	-	-	np	+
9	30 y	M	*MT-ND3*	m.10197G>A	MRI	+	+	-	+	+	(£)	-	-	-	-	-	-	-	-	-	+	-	np	np
10	24 y	M	*MT-ND5*	m.13091T>C	MRI	+	-	-	-	-	(£)	-	-	-	-	+	-	+	+	+	+	-	+	np
11	11 mo	M	*MT-ND5*	m.13513G>A	CT-Scan/MRI	+	+	-	+	+	-	-	-	-	-	-	-	-	+	-	-	-	np	np
12	18 mo	M	*MT-ND5*	m.13513G>A	MRI	+	+	+	-	-	(£)	-		-	-	-	-	-	+	-	-	-	np	+
13	3 y	M	*MT-ND5*	m.13513G>A	MRI	+	+	-	+	+	(£)	-	-	-	-	-	-	-	+	-	-	-	np	+
14	7 y	F	*MT-ND5*	m.13513G>A	MRI	+	-	+	-	-	(£)	-	-	-	-	+	-	+	-	+	+	-	np	+
15	7,5 y	M	*MT-ND5*	m.13513G>A	CT-Scan	+	-	+	-	-	-	($)	-	-	-	-	-	-	-	-	-	-	np	np
16	13 y	F	*MT-ND5*	m.13513G>A	MRI	+	-	-	-	-	(£)	-	-	-	-	-	-	+	-	+	+	-	np	+
17	16 y	M	*MT-ND5*	m.13513G>A	MRI	+	+	+	+	-	(£)	-	-	-	-	-	-	na	na	na	na	-	np	np
18	6 y	M	*MT-ND5*	m.13514A>G	MRI	+	+	+	+	-	(£)	-	-	-	-	-	-	+	-	+	+	-	np	np
19	14 y	M	*MT-ND5*	m.13514A>G	MRI	+	+	-	+	+	(£)	-	-	-	-	-	-	-	-	-	-	-	np	np
20	2 y	M	*MT-ND6*	m.14487T>C	CT-Scan	+	+	+	+	-	-	($)	-	-	-	+	+	-	-	-	-	-	np	np
21	2 mo	M	*NDUFS1*	R241W and R557X	MRI	+	+	-	-	-	(£)	-	-	-	-	-	-	-	-	-	-	-	np	np
22	4 mo	M	*NDUFS1*	R252G and I222del	MRI	+	+	-	-	-	(£)	-	+	- (?)	-	-	-	-	+	-	-	-	np	np
23	6 mo	M	*NDUFS1*	M707V and deletion entire gene	MRI	+	+	-	-	-	(£)	-	+	+ (?)	-	-	+	-	+	+	-	-	np	np
24	8 mo	M	*NDUFS1*	V228A and R252G	MRI	+	-	-	+	-	(£)	-	+	+ (?)	-	-	-	-	+	+	-	-	+	+
25	10 y	M	*NDUFS3*	T145I and R199W	MRI	+	+	+	-	-	(£)	-	+	+	-	-	-	-	-	-	-	-	np	np
26	4 mo	M	*NDUFS4*	D60fs homozygous	MRI	+	+	-	+	-	(£)	-	-	-	-	-	-	-	-	-	-	-	np	+
27	11 mo	M	*NDUFS4*	D119H and K154fs	MRI	+	-	-	+	-	(£)	-	-	-	-	-	-	-	-	-	-	-	np	np
28	2 y	M	*NDUFS4*	W97fs and S159fs	MRI	+	-	-	-	-	(£)	-	-	-	-	-	-	-	+	-	-	-	np	np
29	11 y	F	*NDUFS7*	R145H homozygous	MRI	+	+	-	+	+	(£)	-	+	+	-	-	-	-	-	-	-	-	+	np
30	22 mo	M	*NDUFV1*	Y204C and C206G	MRI	+	+	-	+	-	(£)	-	-	-	-	-	-	-	+	-	-	-	np	np
Total					Brain images	30/30	23/30	11/30	16/30	10/30	0/3	0/28	5/30	4/30	0/30	8/30	6/30	5/29	11/29	7/29	9/29	0/30	3/3	10/10

Abbreviations: mo: month, y: year, M: male, F: female, np: not performed, na: not available, + hypersignal, - normal, C calcifications, # Hyposignal, (?) FLAIR not performed, (£) CT-Scan not performed, ($) MRI not performed

Table 2

	Total (Complex I)	mtDNA (Complex I)	nDNA (Complex I)	mtDNA versus nDNA	
				p value *	conclusion
number of patients	30	20	10	-	-
Mean age at MRI/CT-scan	**6.8 y (2 mo-30 y)**	**8.9 y (4 mo-30 y)**	**2.8 y (2 mo-11 y)**	**0.012**	**s (p<0.05)**
sex ratio (M/F)	5 (25/5)	4 (16/4)	9 (9/1)	0.6	ns
patients < 5 y at time of brain imaging	16	8	8	-	-
patients > 5 y at time of brain imaging	14	12	2	-	-
brainstem	30/30	20/20	10/10	1	ns
putamen	23/30	16/20	7/10	0.6	ns
caudate	**11/30**	**10/20**	**1/10**	**0.049**	**s (p<0.05)**
pallidum	16/30	11/20	5/10	1	ns
putamen or caudate or pallidum	27/30	18/20	9/10	1	ns
brainstem and [putamen or caudate or pallidum]	27/30	18/20	9/10	1	ns
thalamus	10/30	9/20	1/10	0.1	ns
thalamus and [putamen or caudate or pallidum]	**10/30**	**9/20**	**9/10**	**0.02**	**s (p<0.05)**
brainstem and isolated thalamus	0/30	0/20	0/20	1	ns
calcifications in basal ganglia (CT-scan)	0/3	0/3	na	-	-
dilated wirshow robin in basal ganglia (MRI)	0/28	0/18	0/10	-	-
leukoencephalopathy	**5/30**	**0/20**	**5/10**	**0.002**	**s (p<0.01)**
delayed myelinisation	0/30	0/20	0/10	1	ns
stroke-like	**8/30**	**8/20**	**0/10**	**0.03**	**s (p<0.05)**
cortical atrophy	6/30	5/20	1/10	0.6	ns
cerebellum signal hypersignal abnormalities	13/29	8/19	5/10	0.7	ns
cerebellum: hypersignal in cortex	6/29	6/20	0/10	0.07	ns
cerebellum: hypersignal in dentate nucleus	11/29	6/20	5/10	0.4	ns
cerebellum: hypersignal in white matter	7/29	6/20	2/10	0.7	ns
cerebellar atrophy (all ages)	**9/29**	**9/19**	**0/10**	**0.011**	**s (p<0.05)**
cerebellar atrophy when < 5 y	0/16	0/8	0/8	1	ns
cerebellar atrophy when > 5 y	9/14	9/12	0/2	0,1	ns
corpus callosum abnormalities	0/30	0/20	0/10	1	ns
spinal cord	3/3	1/1	2/2	1	ns
lactate (MRS)	10/10	8/8	2/2	1	ns

* Fisher's exact test, Chi2 test or Student t test were used for comparation between mtDNA and nDNA

Abbreviations: mo: month, y: year, na: not available, s: significant, ns: not significant

Table 3

						Brain imaging anomalies																				
Patient	Age at brain imaging	Sex (M/F)	Gene	Mutation	CT-Scan/MRI	brainstem	putamen	caudate	pallidum	thalamus	calcifications in basal ganglia	dilated wirshow robin in basal ganglia	leukoencephalopathy	necrotizing leukoencephalopathy	delayed myelination	stroke-like	cortical atrophy	cerebellum: hypersignal in cortex	cerebellum: hypersignal in dentate nucleus	cerebellum: hypersignal in white matter	cerebellar cortex atrophy	corpus callosum abnormalities	corpus callosum: thin	corpus callosum dysmorphy	Spinal cord	lactate (MRS)
1	4 mo	F	*PDHA1*	c.1153_1158del6	MRI	-	+	-	+	+	(£)	-	-	-	-	-	-	-	-	-	-	+	+	+	np	+
2	2.3 y	M	*PDHA1*	P217R	MRI	-	-	-	+	-	(£)	-	-	-	-	-	-	-	-	-	-	+	-	+	np	-
3	2.3 y	M	*PDHA1*	R378C	MRI	+	+	+	+	+	(£)	-	-	-	+	-	-	na	na	na	+	na	na	na	np	np
4	3y	M	*PDHA1*	Y161Y	MRI	-	-	-	-	-	(£)	-	-	-	+	-	-	-	+	-	+	+	-	+	np	+
5	3.5 y	F	*PDHA1*	R127Q	MRI	-	-	-	-	-	(£)	-	-	-	-	-	-	-	-	-	-	+	+	-	np	-
6	5 y	M	*PDHA1*	IVS7+26G>A	MRI	-	-	-	+	+	(£)	-	-	-	-	-	-	-	+	-	-	-	-	-	np	-
7	2y	M	*PDHX*	c.965-1G>A homozygous	MRI	-	-	-	-	-	(£)	-	-	-	-	-	-	-	-	-	-	+	+	-	np	+
8	3.5 y	M	*PDHX*	R476X homozygous	MRI	+	-	-	-	-	(£)	-	-	-	+	-	-	-	-	-	+	+	+	-	np	+
9	6y	M	*PDHX*	Q248X	MRI	-	-	-	+	-	(£)	-	-	-	-	-	-	-	-	-	-	+	+	-	np	np
10	8y	M	*PDHX*	c.1182+2T>C homozygous	MRI	-	-	-	+	-	(£)	-	-	-	-	-	-	-	-	-	-	+	-	+	np	-
11	9y	F	*PDHX*	c.160+1G>A-c.965-1G>A	MRI	-	-	-	+	-	(£)	-	-	-	-	-	-	-	-	-	-	+	+	+	np	np
Total					Brain images	2/11	2/11	1/11	7/11	3/11	-	0/11	0/11	0/11	3/11	0/11	0/11	0/10	2/10	0/10	3/10	9/10	6/10	4/10	-	4/8
1	4y	M	*MT-TL1*	m.3243A>G	CT-Scan	($)	($)C	($)C	($)C	($)	+	($)	-	-	-	-	-	($)	($)	($)	+	-	-	-	np	np
2	7y	M	*MT-TL1*	m.3243A>G	MRI	-	-	-	-	-	(£)	-	-	-	-	-	-	-	-	-	-	-	-	-	np	-
3	11y	F	*MT-TL1*	m.3243A>G	CT-Scan/MRI	-	-	-	-C	-	+	-	-	-	-	+	-	-	-	-	+	-	-	-	np	np
4	14y	F	*MT-TL1*	m.3243A>G	MRI	-	-	-	-	-	(£)	+	-	-	-	+	+	-	-	-	+	-	-	-	np	np
5	14y	M	*MT-TL1*	m.3243A>G	CT-Scan	($)	($)C	($)	C	($)	+	($)	-	-	-	+	+	($)	($)	($)	+	-	-	-	np	np
6	16y	M	*MT-TL1*	m.3243A>G	CT-Scan	($)	($)C	($)C	($)C	($)	+	($)	-	-	-	-	-	($)	($)	($)	-	-	-	-	np	np
7	22y	F	*MT-TL1*	m.3243A>G	CT-Scan	($)	($)C	($)	($)C	($)	+	($)	-	-	-	+	+	($)	($)	($)	+	-	-	-	np	np
8	55y	M	*MT-TL1*	m.3243A>G	CT-Scan/MRI	-	-	-	-C	-	+	+	-	-	-	-	+	-	-	-	+	-	-	-	np	-
9	56y	F	*MT-TL1*	m.3243A>G	MRI	-	-	-	-	-	(£)	+	-	-	-	-	+	-	-	-	+	-	-	-	np	+
10	20y	F	*MT-TL1*	m.3271 T>C	MRI	-	-	-	-	-	(£)	-	-	-	-	+	-	-	-	-	+	-	-	-	np	np
Total					Brain images	0/6	0/6	0/6	0/6	0/6	6/6	3/5	0/10	0/10	0/10	5/11	5/11	0/6	0/6	0/6	8/11	0/11	0/11	0/11	-	1/3

Abbreviations: mo: month, y: year, M: male, F: female, np: not performed, na: not available, + hypersignal, - normal, C calcifications, # Hyposignal, (?) FLAIR not performed, (£) CT-Scan not performed, ($) MRI not performed

Table 4

	Complex I	PDH	Complex I versus PDH		*MT-TL1*	Complex I versus *MT-TL1*	
			p value *	conclusion		*p value* *	conclusion
number of patients	30	11	-	-	10	-	-
Mean age at MRI/CT-scan	6.8 y (2 mo-30 y)	4.08 y (4 mo-9y)	0.09	ns	21.9 y (4-56y)	0.03	**s (p<0.05)**
sex ratio (M/F)	5 (25/5)	2.66 (8/3)	0.6	ns	1 (5/5)	0.09	ns
patients < 5 y at time of brain imaging	16	7	-	-	1	-	-
patients > 5 y at time of brain imaging	14	4	-	-	9	-	-
brainstem	30/30	2/11	0.0000002	**s (p<0.001)**	0/6	0.0000005	**s (p<0.001)**
putamen	23/30	2/11	0.0012	**s (p<0.01)**	0/6	0.0009	**s (p<0.001)**
caudate	11/30	1/11	0.13	ns	0/6	0.15	ns
pallidum	16/30	7/11	0.7	ns	0/6	0.024	**s (p<0.05)**
putamen or caudate or pallidum	27/30	8/11	0.3	ns	0/6	0.00004	**s (p<0.001)**
brainstem and [putamen or caudate or pallidum]	27/30	1/11	0.000003	**s (p<0.001)**	0/6	0.00004	**s (p<0.001)**
thalamus	10/30	3/11	1	ns	0/6	0.16	ns
thalamus and [putamen or caudate or pallidum]	10/30	3/11	1	ns	0/6	0.16	ns
brainstem and isolated thalamus	0/30	0/11	1	ns	0/6	1	ns
calcifications in basal ganglia (CT-scan)	0/3	-	-	-	6/6	0.012	**s (p<0.05)**
dilated wirshow robin in basal ganglia (MRI)	0/28	0/11	1	ns	3/5	0.0018	**s (p<0.01)**
leukoencephalopathy	5/30	0/11	0.3	ns	0/10	0.3	ns
delayed myelinisation	0/30	3/11	0.015	**s (p<0.05)**	0/10	1	ns
stroke-like	8/30	0/11	0.08	ns	5/11	0.3	ns
cortical atrophy	6/30	0/11	0.17	ns	5/11	0.13	ns
cerebellum signal hypersignal abnormalities	13/29	2/10	0.26	ns	0/6	0.06	ns
cerebellum: hypersignal in cortex	6/29	0/10	0.31	ns	0/6	0.6	ns
cerebellum: hypersignal in dentate nucleus	11/29	2/10	0.45	ns	0/6	0.14	ns
cerebellum: hypersignal in white matter	7/29	0/10	0.16	ns	0/6	0.3	ns
cerebellar atrophy (all ages)	9/29	3/10	1	ns	8/11	0.031	**s (p<0.05)**
cerebellar atrophy when < 5 y	0/16	3/7	0.02	**s (p<0.05)**	1/1	0.059	ns
cerebellar atrophy when > 5 y	9/14	0/4	0.08	ns	7/10	1	ns
corpus callosum dysmorphy	0/30	9/10	0.00000004	**s (p<0.001)**	0/11	1	ns
spinal cord	3/3	-	-	-	-	-	-
lactate (MRS)	10/10	4/8	0.023	**s (p<0.05)**	1/3	0.039	**s (p<0.05)**

* Fisher's exact test, Chi2 test or Student t test were used for comparation between groups

Abbreviations: mo: month, y: year, na: not available, s: significant, ns: not significant

Figure 1

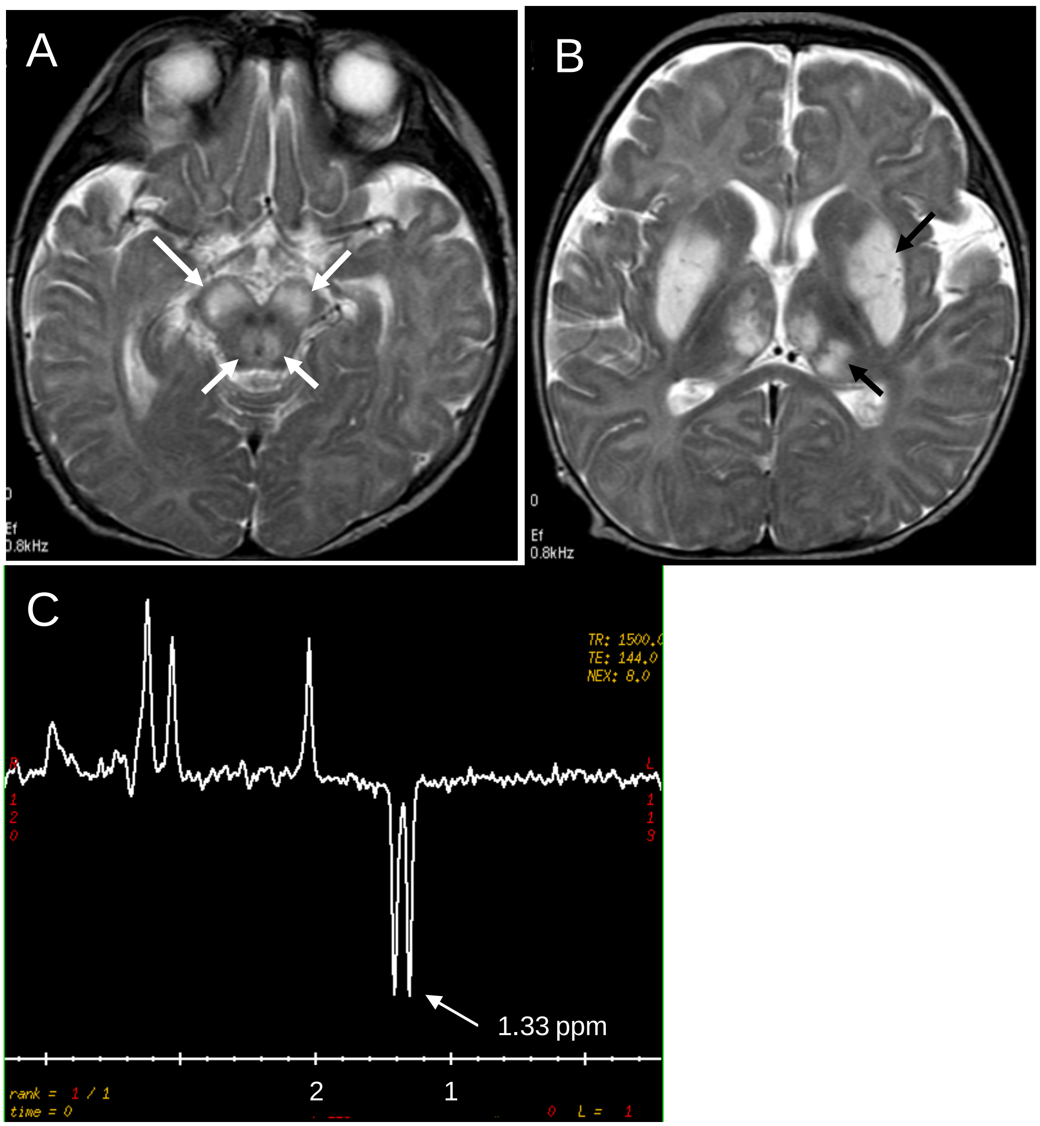

Figure 2